Persistence and Lifelong Fidelity of Phase Singularities in Optical Random Waves

De Angelis, Lorenzo; Alpeggiani, Filippo; Di Falco, Andrea; Kuipers, Kobus

Important note
To cite this publication, please use the final published version (if applicable).
Please check the document version above.

Persistence and lifelong fidelity of phase singularities in optical random waves

L. De Angelis,[1, 2] F. Alpeggiani,[1, 2] A. Di Falco,[3] and L. Kuipers[1, 2]

[1]*Kavli Institute of Nanoscience, Delft University of Technology, 2600 GA, Delft, The Netherlands*

[2]*Center for Nanophotonics, AMOLF, Science Park 104 1098 XG Amsterdam, The Netherlands*

[3]*SUPA, School of Physics and Astronomy, University of St Andrews, North Haugh, St Andrews KY16 9SS, UK*

(Dated: October 4, 2017)

NANOFABRICATION

The chaotic cavity was fabricated on silicon on insulator platform, with a 220 nm thick layer of silicon on a 2 μm thick silica buffer. A 350 nm thick layer of photoresist (ZEP) was deposited via spin coating and baked at 180° C for 10 min. The photonic crystal pattern was exposed with a RAITH e-line electron beam system at 30 kV, developed at 23° C for 45 s in Xylene and transferred onto the silicon layer via reactive ion etching, using a SF_6/CHF_3 balanced gas blend. The samples was then cleaved for measurement via end fire coupling. To this extent, we fabricated in and out-coupling channel waveguides, as sketched in Fig. 1a of the main text.

NEAR-FIELD MICROSCOPY

We map the in-plane components of the optical field in the chaotic cavity with a custom built near-field microscope [1, 2]. The near field is locally sensed with an aperture-type near-field probe, and delivered to the far field through an optical fiber. The probe itself consists of a tapered optical fiber, the tip of which is coated with an approximately 100 nm thick layer of aluminum, and then truncated (aperture size $\sim$ 200 nm). A heterodyne detection scheme enables the measurement of amplitude and phase [3]. With polarization optics we selectively detect the (E_x, E_y) Cartesian components of the in-plane electric field **E** [2, 4, 5]. By scanning the surface of the sample we measure a two-dimensional map of the in-plane complex optical field above the cavity.

SINGULARITIES TRACKING

We track the singularities as a function of wavelength shift with a heuristic algorithm based on the vicinity of singularities in two consecutive frames. In particular, singularities existing in the field have two options: propagation or annihilation (creation). Therefore, all the singularities need to be connected to their propagation in the next frame or to their annihilation/creation partner in the same frame. We establish such connection within an error < 1%. A small amount of trajectories is truncated at the edges of the measured map ($\sim$ 1%). We simply do not consider this trajectories, with no significant consequences on our statistics. A significant amount of trajectories is truncated at the beginning and end of our wavelength sweep. We do not consider these trajectories as well, but we need to take this fact into account, as explained in the main text.

EXPERIMENT REPEATABILITY

We performed the entire wavelength sweep necessary to study the statistics of singularities with different wavelength steps. This was a particularly powerful tool to exclude any experimental artifact which is time-dependent.
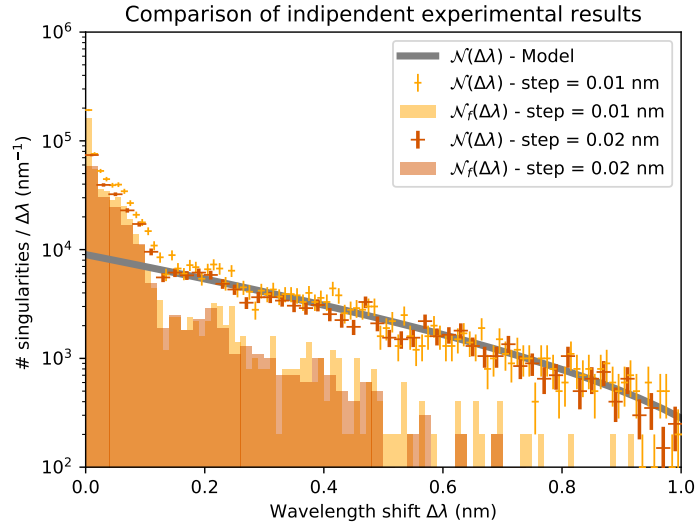
FIG. 1. Persistence histogram with fidelity. The plot is analogous to those reported in Fig. 3(a,b) of the main text. Here we compare the outcome of two independent measurements performed with different wavelength steps. The number of singularities on the y axis is normalized with the wavelength step, in order to allow a direct comparison of the two sets of data.

With different wavelength step indeed any time-dependent effect would turn into a frame-dependent one rather than wavelength shift dependent. In Fig 1 we directly compare measurements performed with steps of 0.01 nm and 0.02 nm, and acknowledge perfect consistency.

NUMERICAL SIMULATIONS

We determine the average loss rate of the system from a three-dimensional FDTD simulation of the chaotic cavity, including the surrounding photonic crystal. The electromagnetic field is excited with a current source located inside the cavity and the loss rate is estimated from the relation

$$\gamma \simeq \frac{\int_{\partial D} d^2\mathbf{r} \, \mathrm{Re}[\mathbf{E}(\mathbf{r}) \times \mathbf{H}^*(\mathbf{r})]}{\int_D d^3\mathbf{r} \, \varepsilon_0 \varepsilon(\mathbf{r})|\mathbf{E}(\mathbf{r})|^2 + \mu_0|\mathbf{H}(\mathbf{r})|^2}, \tag{1}$$

where the numerator and denominator represent the time-averaged energy flux leaving the computational domain D and the total electromagnetic energy inside the domain, respectively. This rate includes both losses due to light escaping into the coupling waveguides and scattering at the photonic-crystal edge.

The value of the electric field $\mathbf{E}(\mathbf{r}, \omega)$ inside the cavity with varying frequency is calculated with a simplified two-dimensional geometry. We assume that the field can be factorized into the form

$$\mathbf{E}(\mathbf{r}) = \mathbf{E}^{(2D)}(x, y)\mathcal{E}_{\mathrm{TE}}(z), \tag{2}$$

where $\mathcal{E}_{\mathrm{TE}}(z)$ is the z-profile of the TE guided mode of a 220 nm silicon-on-insulator slab ($\hat{\mathbf{z}}$ is the out-of-plane direction) and $\mathbf{E}^{(2D)}(x, y)$ is a two-dimensional in-plane polarized field that satisfies the Helmholtz equation with the effective wavenumber $k_{\mathrm{TE}}(\omega)$, which can be obtained by inverting the dispersion relation of the TE guided mode. We simulate $\mathbf{E}^{(2D)}$ by the finite element method on a two-dimensional domain with the same shape as the chaotic cavity. On the boundary of the cavity, we set impedance boundary conditions for an effective band-gap optical material with the dielectric constant $\varepsilon = \varepsilon' + i\varepsilon''$ ($\varepsilon' < 0$), where ε'' is chosen so as to reproduce the loss rate of the three-dimensional FDTD simulations. Please note that such three-dimensional FDTD calculations were computationally

very demanding, and not suitable for efficient wavelength-resolved simulations, which, with the required spectral resolution, required few weeks to be completed. However, we did perform a preliminary FDTD simulation of the full wavelength sweep, and this did not show any qualitative difference with the correspondent FEM simulation. For this reason we then used the FEM simulations, which were by about two orders of magnitude more efficient and gave us more flexibility in tuning different parameters.

COEXISTENCE OF TWO FAMILIES OF EIGENSTATES

Here we present an investigation of the situation in which a second family of eigenstates is added to the decomposition described in Eq. (2) of the main text. This second family is characterized by eigenstates with a spectral width γ', and lies in between the eigenstates of the first family (spectral width γ), i.e.,

$$E_x(\mathbf{r}, \omega) = \sum_j \frac{\mathcal{E}_x^j(\mathbf{r}, \omega_j)}{\omega - (\omega_j + i\gamma)} + \sum_l \frac{\gamma'/\gamma \, \mathcal{E}_x^l(\mathbf{r}, \omega_l)}{\omega - (\omega_l + \Delta/2 + i\gamma')}. \tag{3}$$

Coherently to what described in the main text, the eigenstates of both families are equally spaced ($\omega_{j+1} - \omega_j = \Delta$), and their weight α_j has been set to unity. In this particular example we use $\gamma \approx 4\gamma'$.

In Fig. 2a we show the persistence histogram for the singularities of the field described in Eq. (3). We see that a deviation from a single exponential distribution takes place in the region $\Delta\lambda < 0.2$ nm. Moreover, from the same figure we observe that the number of faithful singularities increases when $\Delta\lambda$ approaches zero, as observed in the experiment. Figure 2b presents the wavelength-wavelength correlation coefficient of the field calculated according to Eq. (3). This is also qualitatively comparable with what reported from the experiment described in the main text.
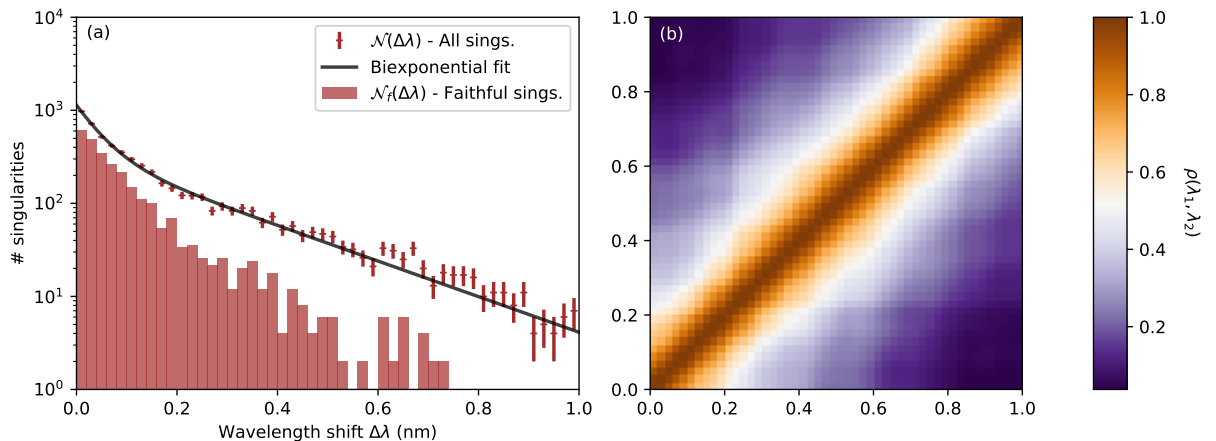

FIG. 2. (a). Persistence histogram with fidelity for the field modeled according to Eq. (3), with $\gamma = 4\gamma'$. The plot is analogous to those reported in Fig. 3(a,b) of the main text. Here, a biexponential fit (black line) highlights the deviation from single exponential distribution. (b). Wavelength-wavelength correlation function for the same field used in the panel (a). The correlation coefficient is calculated as explained in the main text.

[1] C. Liu, R. E. C. van der Wel, N. Rotenberg, L. Kuipers, T. F. Krauss, A. Di Falco, and A. Fratalocchi, Nat. Phys. **11**, 358 (2015).
[2] L. De Angelis, F. Alpeggiani, A. Di Falco, and L. Kuipers, Phys. Rev. Lett. **117**, 093901 (2016).

[3] M. L. M. Balistreri, J. P. Korterik, L. Kuipers, and N. F. van Hulst, Phys. Rev. Lett. **85**, 294 (2000).

[4] M. Burresi, R. J. P. Engelen, A. Opheij, D. van Oosten, D. Mori, T. Baba, and L. Kuipers, Phys. Rev. Lett. **102**, 033902 (2009).

[5] B. Le Feber, N. Rotenberg, D. M. Beggs, and L. Kuipers, Nat. Photonics **8**, 43 (2014).